

Visualization of sphere and horosphere packings related to Coxeter tillings generated by simply truncated orthoschemes with parallel faces

Arnasli Yahya, Jenő Szirmai

Budapest University of Technology and Economics, Institute of Mathematics,
Department of Geometry
Budapest, P. O. Box: 91, H-1521

October 28, 2021

Abstract

In this paper we describe and visualize the densest ball and horoball packing configurations belonging to the simply truncated 3-dimensional hyperbolic Coxeter orthoschemes with parallel faces using the results of [46]. These beautiful packing arrangements describe and show the very interesting structure of the mentioned orthoschemes and the corresponding Coxeter groups. We use for the visualization the Beltrami-Cayley-Klein ball model of 3-dimensional hyperbolic space \mathbb{H}^3 and the pictures were made by the Python software.

1 Introduction

Visualization of mathematical problems is not only a representation of specific objects or an approach in the teaching process, but also plays an important role in understanding the problem and developing solution steps. It can be shown the deeper contexts of the problem and the possibilities for moving forward.

In hyperbolic spaces \mathbb{H}^n for $2 \leq n \leq 9$, the known densest ball and horoball configurations are derived by Coxeter simplex tilings, therefore it is interesting to

determine their optimal horoball packings related to Coxeter tilings. In the former papers, we investigated that Coxeter simplex tilings whose generating simplices do not have parallel faces. In [46] we extended our study to the 3 dimensional Coxeter tilings generated by simple frustum orthoschemes with parallel faces. But first, we recall some results related to the above topic.

In the case of periodic ball or horoball packings, this local density defined above can be extended to the entire hyperbolic space and is related to the simplicial density function (defined below) that we generalized in [31] and [32]. In this paper, we shall use such definition of packing density.

A Coxeter simplex is a top dimensional simplex in $\overline{\mathbb{H}}^n$ with dihedral angles either integral submultiples of π or zero. The group generated by reflections on the sides of a Coxeter simplex is a Coxeter simplex reflection group. Such reflections generate a discrete group of isometries of \mathbb{H}^n with the Coxeter simplex as the fundamental domain; hence the groups give regular tessellations if the fundamental simplex is characteristic. We note here that the Coxeter groups are finite for \mathbb{S}^n , and infinite for \mathbb{E}^n or $\overline{\mathbb{H}}^n$.

There are non-compact Coxeter simplices in $\overline{\mathbb{H}}^n$ with ideal vertices in $\partial\mathbb{H}^n$, however only for dimensions $2 \leq n \leq 9$; furthermore, only a finite number exists in dimensions $n \geq 3$. Johnson *et al.* [16] found the volumes of all mentioned Coxeter simplices in hyperbolic n -space, also see Kellerhals [18]. Such simplices are the most elementary building blocks of hyperbolic manifolds, the volume of which is an important topological invariant.

In n -dimensional space of constant curvature ($n \geq 2$), define the simplicial density function $d_n(r)$ to be the density of $n + 1$ mutually tangent balls of radius r in the simplex spanned by their centers. L. Fejes Tóth and H. S. M. Coxeter conjectured that the packing density of balls of radius r in X cannot exceed $d_n(r)$. Rogers [29] proved this conjecture in Euclidean space \mathbb{E}^n . The 2-dimensional spherical case was settled by L. Fejes Tóth [11], and Böröczky [7], who extend the analogous statement to n -dimensional spaces of constant curvature.

The simplicial packing density upper bound $d_3(\infty) = (1 + \frac{1}{2^2} - \frac{1}{4^2} - \frac{1}{5^2} + \frac{1}{7^2} + \frac{1}{8^2} - - + \dots)^{-1} = 0.85327\dots$ cannot be achieved by packing regular balls, instead it is realized by horoball packings of $\overline{\mathbb{H}}^3$, the regular ideal simplex tiles $\overline{\mathbb{H}}^3$. More precisely, the centers of horoballs in $\partial\overline{\mathbb{H}}^3$ lie at the vertices of the ideal regular Coxeter simplex tiling with Schläfli symbol $\{3, 3, 6\}$.

In [20] we proved that this optimal horoball packing configuration in \mathbb{H}^3 is not unique. We gave several more examples of regular horoball packing arrangements based on asymptotic Coxeter tilings using horoballs of different types, that

is horoballs that have different relative densities with respect to the fundamental domain, that yield the Böröczky–Florian-type simplicial upper bound [8].

Furthermore, in [31, 32] we found that by allowing horoballs of different types at each vertex of a totally asymptotic simplex and generalizing the simplicial density function to $\overline{\mathbb{H}}^n$ for $(n \geq 2)$, the Böröczky-type density upper bound is not valid for the fully asymptotic simplices for $n \geq 4$. For example, in $\overline{\mathbb{H}}^4$ the locally optimal simplicial packing density is $0.77038\dots$, higher than the Böröczky-type density upper bound of $d_4(\infty) = 0.73046\dots$ using horoballs of a single type. However these ball packing configurations are only locally optimal and cannot be extended to the entirety of the ambient space $\overline{\mathbb{H}}^n$. In [21] we found seven horoball packings of Coxeter simplex tilings in $\overline{\mathbb{H}}^4$ that yield densities of $5\sqrt{2}/\pi^2 \approx 0.71645$, counterexamples to L. Fejes Tóth’s conjecture of $\frac{5-\sqrt{5}}{4}$ stated in his foundational book *Regular Figures* [11, p. 323].

In [22], [23] we extend our study of horoball packings to $\overline{\mathbb{H}}^n$ ($5 \leq n \leq 9$) using our methods that were successfully applied in lower dimensions. In the previously mentioned papers we studied the ball and horoball packing related to the Coxeter simplex tilings where the vertices of the simplices are proper points of the hyperbolic space \mathbb{H}^n or they are ideal i.e. lying on the sphere $\partial\mathbb{H}^n$.

In [46], we considered the Coxeter tilings in 3-dimensional hyperbolic space \mathbb{H}^3 where the generating orthoscheme is a simple truncated Coxeter orthoscheme with parallel faces i.e. their dihedral angle is zero. Here we studied the Coxeter tilings which are given with Schläfli symbol $\{\infty, q, r, \infty\}$ (see Fig. 1. second graph). We determined their optimal ball and horoball packings, proved that the densest packing arrangement of the considered tilings is realized at the tilings $\{\infty, 3, 6, \infty\}$, and $\{\infty; 6; 3; \infty\}$ by horoballs with density ≈ 0.8413392 .

Remark 1.1 *The first cases in Fig. 1. is investigated in papers [38, 39, 40] where from the truncated orthoschemes can be derived prism like tilings generated hyperball or hyp-hor packings (or coverings) in \mathbb{H}^3 .*

In this paper we describe and visualize the densest ball and horoball packing configurations belonging to the simply truncated 3-dimensional hyperbolic Coxeter orthoschemes with parallel faces using the results of [46]. These beautiful packing arrangements describe and show the very interesting structure of the mentioned orthoschemes and the corresponding Coxeter groups. We use for the visualization the Beltrami-Cayley-Klein ball model of 3-dimensional hyperbolic space \mathbb{H}^3 and the pictures were made by the Ipy Volume, a Python library for visualizing 3D-object.

2 Basic Notions

For the computations and visualization, we use the projective model of the hyperbolic space \mathbb{H}^3 . The model is defined in the $\mathbb{E}^{1,n}$ Lorentz space with signature $(1, n)$, i.e. consider \mathbf{V}^{n+1} real vector space equipped with the bilinear form:

$$\langle \mathbf{x}, \mathbf{y} \rangle = -x^0 y^0 + x^1 y^1 + \cdots + x^n y^n.$$

In the vector space, consider the following equivalence relation:

$$\mathbf{x}(x^0, \dots, x^n) \sim \mathbf{y}(y^0, \dots, y^n) \Leftrightarrow \exists c \in \mathbb{R} \setminus \{0\} : \mathbf{y} = c \cdot \mathbf{x}.$$

The factorization with \sim induces the $\mathcal{P}^n(\mathbf{V}^{n+1}, \mathbf{V}_{n+1})$ n -dimensional real projective space. In this space to interpret the points of \mathbb{H}^n hyperbolic space, consider the following quadratic form:

$$Q = \{[\mathbf{x}] \in \mathcal{P}^n \mid \langle \mathbf{x}, \mathbf{x} \rangle = 0\} =: \partial \mathbb{H}^n.$$

The inner points relative to the cone-component determined by Q are the points of \mathbb{H}^n (for them $\langle \mathbf{x}, \mathbf{x} \rangle < 0$), the point of $Q = \partial \mathbb{H}^n$ are called the points at infinity, and the points lying outside relative to Q are outer points of \mathbb{H}^n (for them $\langle \mathbf{x}, \mathbf{x} \rangle > 0$). We can also define a linear polarity between the points and hyperplanes of the space: the polar hyperplane of a point $[\mathbf{x}] \in \mathcal{P}^n$ is $Pol(\mathbf{x}) := \{[\mathbf{y}] \in \mathcal{P}^n \mid \langle \mathbf{x}, \mathbf{y} \rangle = 0\}$, and hence $\mathbf{x} \in \mathbf{V}^{n+1}$ is incident with $\mathbf{a} \in \mathbf{V}_{n+1}$ iff $\mathbf{x} \cdot \mathbf{a} = 0$. In this projective model, we can define a metric structure related to the above bilinear form, where for the distance of two proper points:

$$\cosh \left(\frac{d(\mathbf{x}, \mathbf{y})}{k} \right) = \frac{-\langle \mathbf{x}, \mathbf{y} \rangle}{\sqrt{\langle \mathbf{x}, \mathbf{x} \rangle \langle \mathbf{y}, \mathbf{y} \rangle}}, \quad (\text{at present } k = 1). \quad (2.1)$$

This corresponds to the distance formula in the well-known Beltrami-Cayley-Klein model.

3 The structures of truncated orthoschemes

Our aim to visualize the simply asymptotic orthoschemes that contain parallel hyperplane faces in 3-dimensional hyperbolic space. This orthoschemes are represented by their Coxeter graphs (see Fig.??), where the parameters p, q, r are satisfy the inequalities $\frac{1}{p} + \frac{1}{q} < \frac{1}{2}$ and $\frac{1}{q} + \frac{1}{r} \geq \frac{1}{2}$.

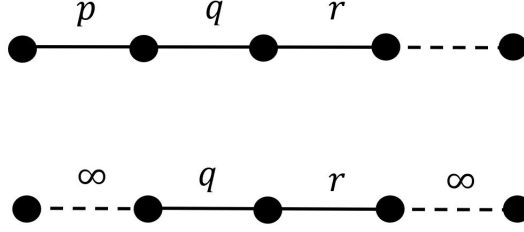


Figure 1: The Coxeter graph

We will study the second type of the orthoschemes that has corresponding Coxeter-Schläfli Matrix as follows

$$C = \begin{bmatrix} 1 & -\cos\left(\frac{\pi}{p}\right) & 0 & 0 & 0 \\ -\cos\left(\frac{\pi}{p}\right) & 1 & -\cos\left(\frac{\pi}{q}\right) & 0 & 0 \\ 0 & -\cos\left(\frac{\pi}{q}\right) & 1 & -\cos\left(\frac{\pi}{r}\right) & 0 \\ 0 & 0 & -\cos\left(\frac{\pi}{r}\right) & 1 & c_4 \\ 0 & 0 & 0 & c_4 & 1 \end{bmatrix}, \quad (3.1)$$

where the constant c_4 can be uniquely determined in the arrangement of Napier cycles [14], i.e .

$$c_4 = -\sqrt{\frac{1 + \cos^2\left(\frac{\pi}{p}\right) \cos^2\left(\frac{\pi}{r}\right) - \cos^2\left(\frac{\pi}{p}\right) - \cos^2\left(\frac{\pi}{q}\right) - \cos^2\left(\frac{\pi}{r}\right)}{1 - \cos^2\left(\frac{\pi}{p}\right) - \cos^2\left(\frac{\pi}{q}\right)}}.$$

In our case, there are two parallel faces (hyperplanes) that meet in an ideal point. That means the dihedral angle between these two hyperplanes is equal to 0. Therefore, we assume that these two hyperplanes are h_0 and h_1 . Thus, their dihedral angle is $w_0 = \frac{\pi}{p} \rightarrow 0$, if p tends to ∞ , the Coxeter-Schläfli matrix (3.1) would change to the following form

$$C = \begin{bmatrix} 1 & -1 & 0 & 0 & 0 \\ -1 & 1 & -\cos\left(\frac{\pi}{q}\right) & 0 & 0 \\ 0 & -\cos\left(\frac{\pi}{q}\right) & 1 & -\cos\left(\frac{\pi}{r}\right) & 0 \\ 0 & 0 & -\cos\left(\frac{\pi}{r}\right) & 1 & -1 \\ 0 & 0 & 0 & -1 & 1 \end{bmatrix} \quad (3.2)$$

We notice that C is a singular matrix. The crucial issue is that the complete orthoscheme is uniquely, up to isometry, determined by the 4×4 -non singular

principal submatrix of C , we write this principal submatrix as $C(p, q, r)$,

$$C(p, q, r) = \begin{bmatrix} 1 & -\cos\left(\frac{\pi}{p}\right) & 0 & 0 \\ -\cos\left(\frac{\pi}{p}\right) & 1 & -\cos\left(\frac{\pi}{q}\right) & 0 \\ 0 & -\cos\left(\frac{\pi}{q}\right) & 1 & -\cos\left(\frac{\pi}{r}\right) \\ 0 & 0 & -\cos\left(\frac{\pi}{r}\right) & 1 \end{bmatrix}. \quad (3.3)$$

By the Proposition 1.6 in [14], one could have a set (unique, up to isometries) of 3+1 unit positive vectors $\mathbf{u}_0, \mathbf{u}_1, \mathbf{u}_2, \mathbf{u}_3$ admitting $C(p, q, r)$ as their Gram matrix and thus generating a Napier cycle in $\mathbb{R}^{1,3}$. Their pols $\mathbf{u}_0, \mathbf{u}_1, \mathbf{u}_2, \mathbf{u}_3$ are the “unit normals” of the hyperplanes h_0, h_1, h_2, h_3 respectively,

$$h_i = \{\mathbf{x} \in \mathbb{R}^{1,3} \mid \langle \mathbf{x}, \mathbf{u}_i \rangle = 0\},$$

for $i = 0, 1, 2, 3$. The matrix A , inverse of matrix $C(p, q, r)$, would uniquely determine the coordinates of the orthoscheme vertices relative to chosen basis vectors $\mathbf{u}_0, \mathbf{u}_1, \mathbf{u}_2, \mathbf{u}_3$. The location of the vertices is completely described by the column of matrix EA , where $E = [\mathbf{u}_0, \mathbf{u}_1, \mathbf{u}_2, \mathbf{u}_3]$, therefore by this observation,

we choose the initial vectors $\mathbf{u}_0 = \begin{bmatrix} \sinh t \\ 0 \\ \cosh t \\ 0 \end{bmatrix}$ and $\mathbf{u}_3 = \begin{bmatrix} 0 \\ 0 \\ 0 \\ 1 \end{bmatrix}$ where the parameter

$t \in \mathbb{R}$. We determine the vectors $\mathbf{u}_1, \mathbf{u}_2$, and \mathbf{u}_4 based on these initial vectors and by the benchmark Coxeter-Schläfli matrix C .

Our result is described in the Beltrami-Cayley-Klein-Sphere model of 3 dimensional hyperbolic space \mathbb{H}^3 , see Fig.2, 3, 4, and 5. In Fig.2, we provide the basic structure of a truncated orthoscheme with two pairs of parallel faces that intersect each other at the infinity. These intersection is described by two tangent lines of the model sphere, k and l . The corresponding Coxeter group is generated by reflections with respect to its faces $h_0(\mathbf{u}_0), h_1(\mathbf{u}_1), h_2(\mathbf{u}_2), h_3(\mathbf{u}_3), h_4(\mathbf{u}_4)$ (admitting the given Gram matrix G). This group can be generated by reflections $\{T_0, T_1, T_2, T_3, T_4\}$, where T_i ($i = 0 \dots 4$) denote the reflection with respect to the hyperplane h_i . The reflections can be described in this model by the following formula:

$$T_i(\mathbf{x}) = \mathbf{x} - 2\langle \mathbf{x}, \mathbf{u}_i \rangle \mathbf{u}_i, \quad \text{where } i = 0, 1, \dots, 4.$$

The computer visualization of the truncated orthoschemes are given in Fig.3, 4, and 5.

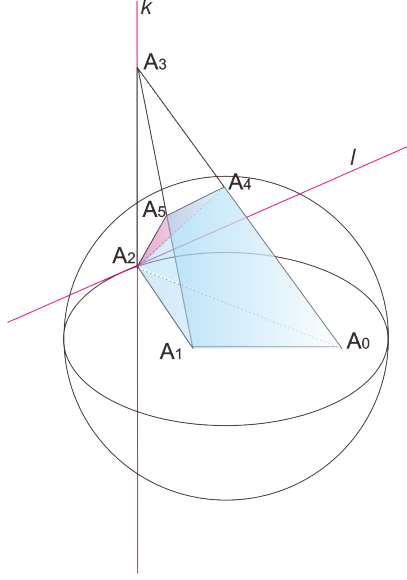


Figure 2: The structure of truncated orthoscheme with the two intersection pairs of its parallel faces.

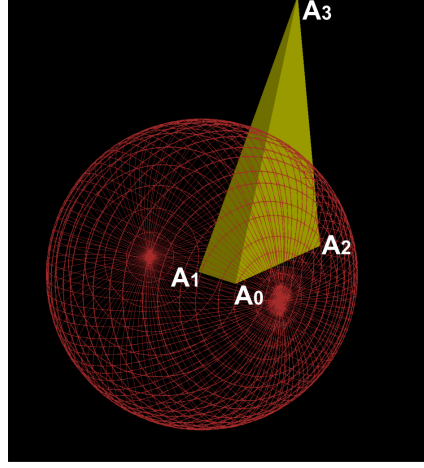


Figure 3: Orthoscheme with a ultra ideal vertex A_3 , and the couple of parallel faces $(A_0A_1A_2A_3$ and $A_1A_2A3A_4)$

4 On sphere packings

In constructing the inball, the largest inscribed classical ball, in the truncated orthoscheme, we follow the procedure of [15], that constructed the inscribed sphere into a polyhedra in hyperbolic spaces \mathbb{H}^n . For $i, j \in \{0, 1, 2, 3\}$, $i \neq j$, let $S_{ij}(\mathbf{s}_{ij})$ be hyperbolic hyperplane given by the following formula where \mathbf{u}_i are the above unit poles (normal vectors) of forms \mathbf{u}_i :

$$\mathbf{s}_{ij} := (\mathbf{u}_i - \mathbf{u}_j)^\perp. \quad (4.1)$$

Basically, the hyperplane $S_{ij}(\mathbf{s}_{ij})$ is a bisector hyperplane that divide the dihedral angle between h_i and h_j into two equal parts. Based on this notion, we construct a set of vectors as follows

$$\mathbf{s}_i = \mathbf{u}_i - \mathbf{u}_{i+1},$$

for $i = 0, 1, 2$. Note that the forms $\mathbf{s}_0, \mathbf{s}_1, \mathbf{s}_2$ are linearly independent in \mathbb{R}^4 . Now, we have three hyperbolic bisector hyperplanes $S_i(\mathbf{s}_i)$, where $i = 0, 1, 2$. Let $\hat{X}(\hat{\mathbf{x}})$

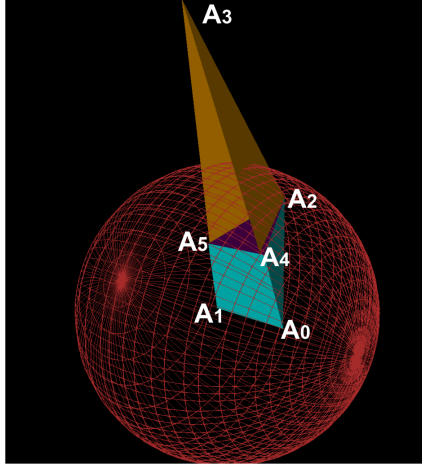


Figure 4: Truncated orthoscheme, where the truncating face $A_2A_4A_5$

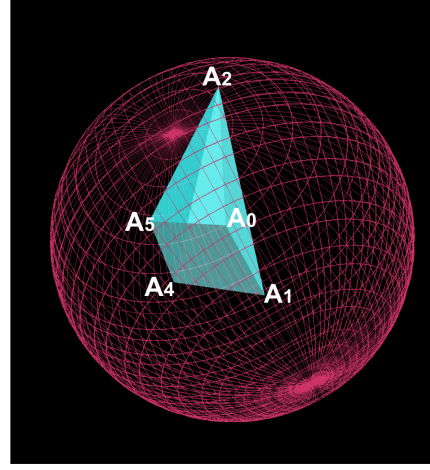


Figure 5: Truncated orthoscheme with the truncating face $A_2A_4A_5$

be the common point of the bisector hyperplanes:

$$\hat{\mathbf{x}} := \bigcap_{i=0,1,2} S_i(\mathbf{s}_i). \quad (4.2)$$

That means, we consider the equations system

$$\langle \hat{\mathbf{x}}, \mathbf{s}_i \rangle = 0, \quad i = 0, 1, 2. \quad (4.3)$$

We consider that solution where $\hat{\mathbf{x}}$ is a proper point in the model and lies in the given orthoscheme. The visualization of optimum inball in truncated orthoscheme $\{\infty, 3, 3, \infty\}$ is given on Fig.6. The problem might be occurred when the inball intersect the truncating hyperplane s_4 (see Fig 7). In that situation, the inradius is greater than the distance between the center of the inball and the truncating hyperplane h_4 , i.e

$$\begin{aligned} r &= d_{\mathcal{H}}(X, h_0) = d_{\mathcal{H}}(X, h_1) = d_{\mathcal{H}}(X, h_2) = d_{\mathcal{H}}(X, h_3) \\ &\geq d_{\mathcal{H}}(X, h_4). \end{aligned}$$

The three bisectors can be re-chosen in such that the inball does not intersect the omitting hyperplane. There are 5 complete combinations of bisectors for constructing the candidate of inball center. The complete packings denisties of inball

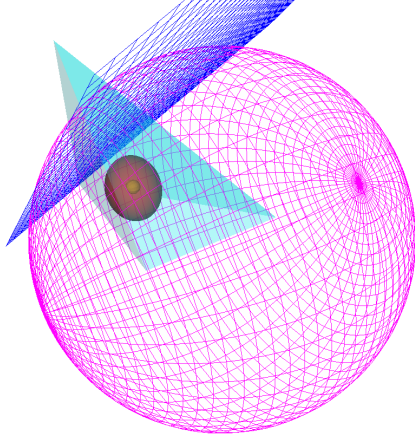


Figure 6: Optimum inball in the truncated orthoscheme $\{\infty, 3, 3, \infty\}$

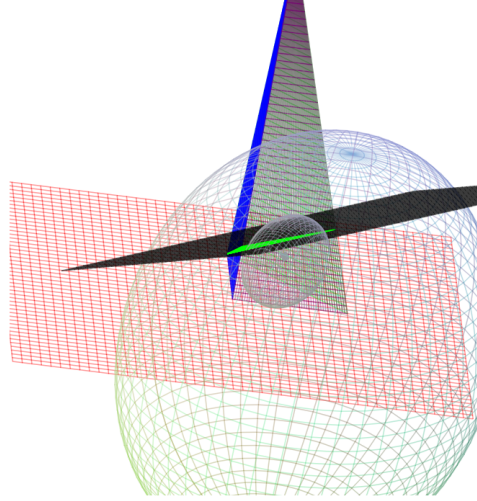


Figure 7: The inball intersects the truncating hyperplane h_4

packing (and their optimum density) can be found in [46], that gave the optimum packing density ≈ 0.2623649 , attained by sphere packing in $(\infty, 3, 3, \infty)$.

5 On horosphere packings

A horosphere in the hyperbolic geometry is the surface orthogonal to the set of parallel lines, passing through the same point on the absolute quadratic surface $\partial\mathbb{H}^n$ (at present $n = 3$) (simply absolute) of the hyperbolic space \mathbb{H}^3 .

We introduce an usual projective coordinate system using vector basis \mathbf{b}_i ($i = 0, 1, 2, 3$) for \mathcal{P}^3 where the coordinates of center of the model is $C = (1, 0, 0, 0)$. We pick an arbitrary point at infinity to be $A_3 = (1, 0, 0, 1)$.

As it is known, the equation of a horosphere with center $A_3 = (1, 0, 0, 1)$ through point $S = (1, 0, 0, s)$ ($s \in (-1, 1)$) is

$$\frac{(s-1)^2}{1-s^2}(-x^0x^0 + x^1x^1 + x^2x^2 + x^3x^3) + (x^0 - x^3)^2 = 0$$

This surface can be described in given usual Cartesian coordinate system by the

following formula

$$\frac{2(x^2 + y^2)}{1 - s} + \frac{4(z - (\frac{s+1}{2}))^2}{(1 - s)^2} = 1, \quad (5.1)$$

where $x = \frac{x^1}{x^0}$, $y = \frac{x^2}{x^0}$, $z = \frac{x^3}{x^0}$.

In computer visualization, it is very powerful to convert the horosphere equation into a polar coordinate system. We use the following conversion

$$x = \sqrt{\frac{1-s}{2}} \cos \theta \sin \phi, \quad y = \sqrt{\frac{1-s}{2}} \sin \theta \sin \phi, \quad z = \frac{1+s}{2} + \frac{1-s}{2} \cos \phi, \quad (5.2)$$

where parameters $\theta \in [0, 2\pi)$, $\phi \in [0, \pi]$.

We will frequently be dealing with the arbitrary coordinate of orthoscheme (based on the set of unit normal Napier cycles). It would be useful if we place our arbitrary ideal point A_2 to $(1, 0, 0, 1)$, by the following ideas. We find the transformation T (depend on two parameters) such that $T(A_2) = (1, 0, 0, 1)$. Basically, this transformation T is represented by a composition two rotations, i.e its representation matrix is described in the form

$$\begin{bmatrix} 1 & 0 & 0 & 0 \\ 0 & \cos(\phi) & -\sin(\phi) & 0 \\ 0 & \sin(\phi) & \cos(\phi) & 0 \\ 0 & 0 & 0 & 1 \end{bmatrix} \begin{bmatrix} 1 & 0 & 0 & 0 \\ 0 & 1 & 0 & 0 \\ 0 & 0 & \cos(\theta) & -\sin(\theta) \\ 0 & 0 & \sin(\theta) & \cos(\theta) \end{bmatrix}.$$

Having the coordinate of ideal points A_2 , one could determine the value of parameters ϕ , and θ . Finally, by using transformation T , we move our truncated orthoscheme such that the ideal vertex A_2 has the coordinates $(1, 0, 0, 1)$. Then one could apply the formulas (5.1), and (5.2) to construct the horosphere equations.

We separate our discussion into two cases depending on the number of vertices lying at infinity. First, we consider that case if the truncated orthoschemes have only one ideal vertex i.e A_2 . In this case, we attach a horosphere centred at ideal vertex, A_2 .

While on the second case we shall consider the situation where two vertices of truncated orthoschemes lie on the absolute they are happened in cases $\{\infty, 3, 6, \infty\}$, $\{\infty, 4, 4, \infty\}$, and $\{\infty, 6, 3, \infty\}$. In each case, we could put a horosphere centered

at either ideal vertex. We can also attach two horospheres altogether, where they are touching each other at edge A_0A_2 .

5.0.1 Packings with one horosphere

We have some truncated orthoschemes given with Schläfli symbols such that it has only one point at the infinity, e.g : $\{\infty, 3, 3, \infty\}$, $\{\infty, 3, 4, \infty\}$, $\{\infty, 3, 5, \infty\}$, $\{\infty, 4, 3, \infty\}$, $\{\infty, 5, 3, \infty\}$. However, if the truncated orthoscheme has two ideal vertices of truncated orthoscheme we can also study the corresponding horosphere packing centered at one either of these vertices.

It is clear that the densest horosphere packing configuration would be reached whenever this horosphere (horoball) with center A_2 touch the opposite face (represented by hyperplane h_2). One could simply take the projection of A_2 onto its opposite face by the projection formula $P_{h_2}(\mathbf{a}_2) = \mathbf{a}_2 - \langle \mathbf{a}_2, \mathbf{u}_2 \rangle \mathbf{u}_2$.

The optimal horosphere should contains the point $P_{h_2}(A_2)$ therefore we can determine the parameter s and so the equation (5.1) of the horosphere.

We provide the computer visualization of optimum horospheres packing, attained by truncated orthoscheme tilings $\{\infty, 3, 3, \infty\}$, in Fig. 8, Fig. 9, and Fig. 10. The optimum packing density is ≈ 0.8188080 , see [46].

5.0.2 Packing with two horospheres

Now, we focus on the orthoscheme tiling with the Schläfli symbol e.g $\{\infty, 3, 6, \infty\}$, $\{\infty, 4, 4, \infty\}$, and $\{\infty, 6, 3, \infty\}$. In these cases given by the above Schläfli symbols, we consider the generating truncated orthoscheme with 2 ideal vertices i.e A_2 and A_0 lie at the infinity. We construct two horospheres centered at A_2 and A_0 . We denote the horospheres centered at A_2 and A_0 with \mathcal{B}_2 and \mathcal{B}_0 , respectively. It is clear, that in the optimal case these horospheres would touch each other at the edge joining A_2 and A_0 , see Fig.(11). The question is at which point of the edge the optimal (densest packing) configuration occurs if we move the touching point along edge joining A_2 and A_0 .

Remark 5.1 : *These two horospheres could not intersect over their opposite faces, therefore there will be a restriction for the movement of the touching point.*

We can parameterize the possible movement of the touching point P , see Fig. 11, e.g. $P(\mathbf{r}(t)) = (1 - t)\mathbf{a}_2 + t \cdot \mathbf{a}_0$. Then, for every possible t , we have parameters

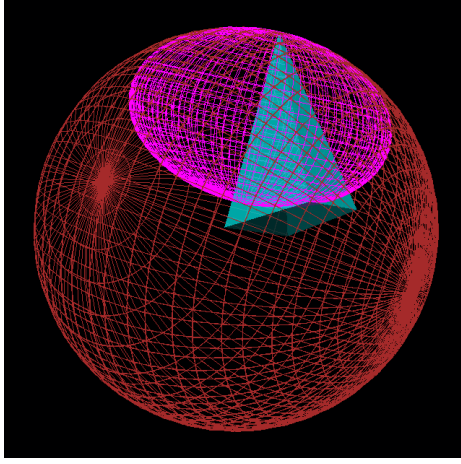


Figure 8: The largest horoball related to truncated orthoscheme of tiling $\{\infty, 3, 3, \infty\}$

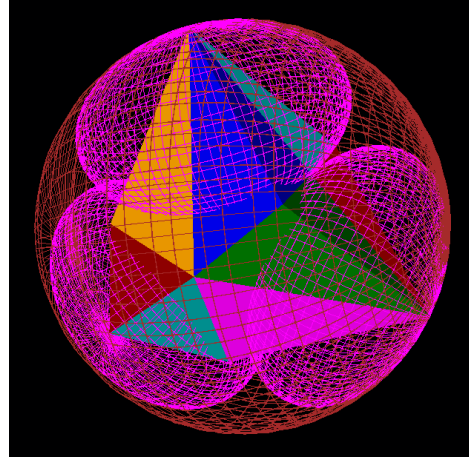


Figure 9: The neighbouring orthoschemes and horospheres configuration (first crown) related to truncated orthoscheme tiling $\{\infty, 3, 3, \infty\}$

s_i ($i = 1, 2$) related to the both horospheres.

Optimal horoball packing of tiling $\{\infty, 4, 4, \infty\}$

In this situation, we have quite interesting structure, we obtain that the possible values of t are $t \in [\approx 0.2150 < t < \approx 0.3497]$. We can compute the volumes of horoball sectors as the functions of t . It is just similar to the previous case, the volume function of horoball sectors centered at A_2 is a monotonic increasing function of t if the touching point moving with direction A_2 to A_0 while the volume function of horoball sectors centered at A_0 is decreasing in this situation.

In this case, we proved (see [46]) that the density is increasing as a function of t , see Fig. 12. Furthermore, the maximum density is attained when t is largest, i.e when the horosphere centered at A_2 touches the opposite face.

$$\delta_{opt}(\mathcal{B}(4, 4, t) = \sup \delta(\mathcal{B}(4, 4, t)) \approx 0.8188081.$$

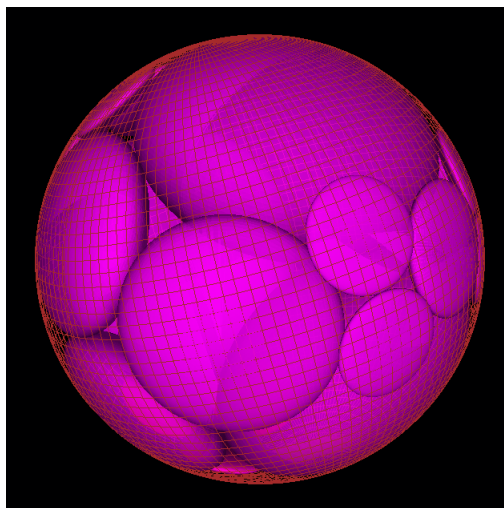


Figure 10: The first-third crowns of neighbouring horosphere configurations related to truncated orthoscheme tiling $\{\infty, 3, 3, \infty\}$

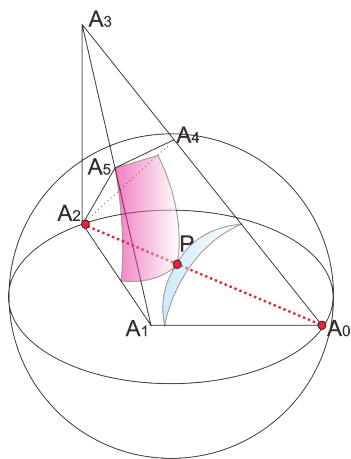


Figure 11: Two horospheres, \mathcal{B}_0 and \mathcal{B}_2 , that touch each other at a point lying on the edge A_0A_2

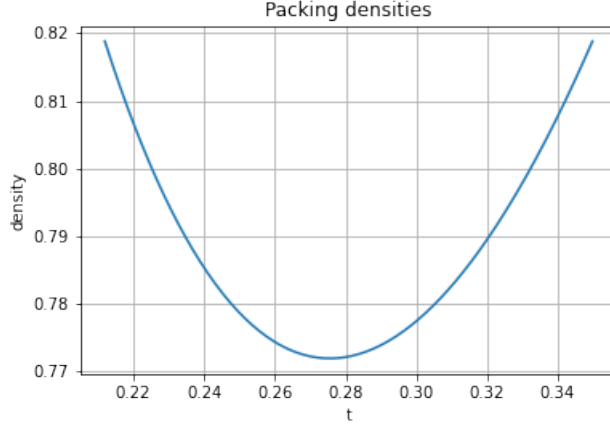


Figure 12: The plot of density function for all possible t in case $\{\infty, 4, 4, \infty\}$

Optimal horoball packing of tilings $\{\infty, 3, 6, \infty\}$ and $\{\infty, 6, 3, \infty\}$

We visualize similarly to the above case the densest horosphere (horoball) packings related to the truncated orthoscheme tilings with Schläfli symbol $\{\infty, 3, 6, \infty\}$ and $\{\infty, 6, 3, \infty\}$. There are some basic facts occurred in the orthoschemes with Schläfli symbol $\{\infty, 3, 6, \infty\}$, $\{\infty, 6, 3, \infty\}$.

1. In this situation, there is in each case only one possible value of parameters t , $t_{(3,6)} \approx 0.2119416$, $t_{(6,3)} \approx 0.5745582$.
2. If $(q, r) = (3, 6)$ then the optimal horosphere \mathcal{B}_2 touches the plane h_2 and \mathcal{B}_0 touches the face h_0 and if $(q, r) = (6, 3)$ \mathcal{B}_2 touches the plane h_2 and \mathcal{B}_0 touches the face h_4 .
3. The packing density of these two configurations are the same, ≈ 0.8413392 , see [46].

Finally, we give the computer visualization in Fig. 13-15 related to Coxeter tiling $\{\infty, 3, 6, \infty\}$ and in Fig. 17-20 for Coxeter tiling $\{\infty, 6, 3, \infty\}$.

In our opinion, non-Euclidean tilings and packings and their investigations will play an important role in the research of material structure in the near future.

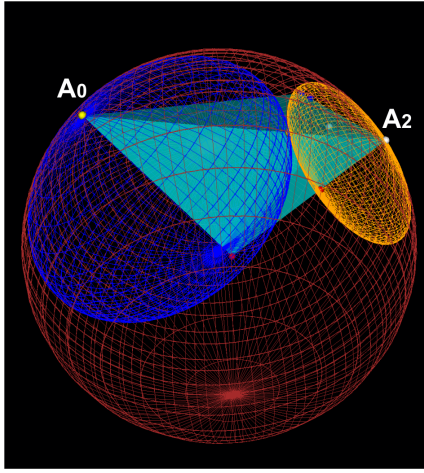


Figure 13: Two horospheres, \mathcal{B}_0 and \mathcal{B}_2 , that touch each other at the point lying on A_0A_2 related to tiling $\{\infty, 3, 6, \infty\}$.

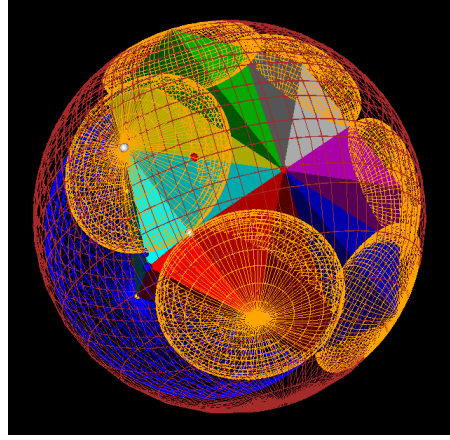


Figure 14: Adjacent orthoschemes and the corresponding horosphere configuration (first crown) related to truncated orthoscheme tiling $\{\infty, 3, 6, \infty\}$

Therefore, we also consider it important to visualize them in order to get to know them.

References

- [1] BEZDEK, K.: Sphere Packings Revisited, *European Journal of Combinatorics*, **27/6** (2006), 864–883.
- [2] BOWEN, L. - RADIN, C.: Optimally Dense Packings of Hyperbolic Space, *Geometriae Dedicata*, (2004) **104**, 37–59.
- [3] BOLYAI, J.: Appendix, *Scientiam Spatii absolute verum exhibens;...*, (1831), Marosvásárhely.
- [4] BÖHM, J. – HERTEL, E: *Polyedergeometrie in n -dimensionalen Räumen konstanter Krümmung*, Birkhäuser, Basel (1981).

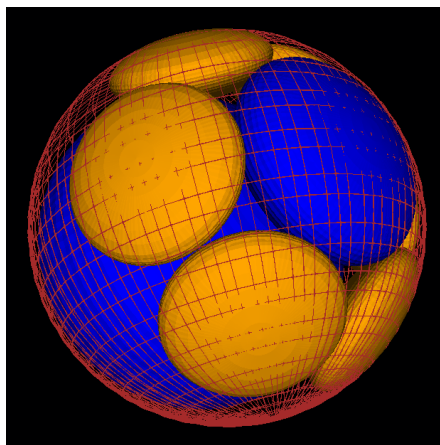


Figure 15: The horosphere configuration (first crown) related to truncated orthoscheme tiling $\{\infty, 3, 6, \infty\}$

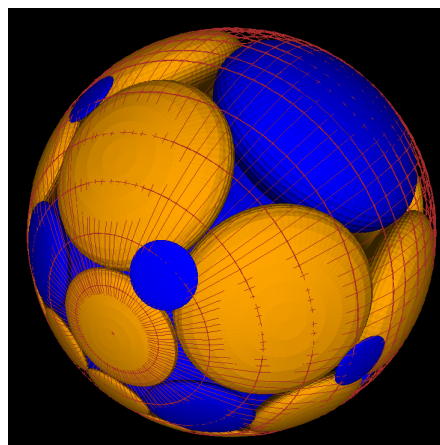


Figure 16: The optimum packing density horospheres configuration (first-third crown) related to the orthoscheme tiling $\{\infty, 3, 6, \infty\}$.

- [5] BÖRÖCZKY, K.: Gömbelhelyezések állandó görbületű terekben I., *Math. Lapok*, **25**, (1974), 265–306.
- [6] BÖRÖCZKY, K.: Gömbelhelyezések állandó görbületű terekben II., *Math. Lapok*, **26**, (1975), 67–90.
- [7] BÖRÖCZKY, K.: Packings of spheres in spaces of constant curvature, *Acta Math. Acad. Sci. Hungar.*, **32**, (1978), 243–261.
- [8] BÖRÖCZKY, K. – FLORIAN, A.: Über die dichteste Kugelpackung im hyperbolischen Raum, *Acta Math. Acad. Sci. Hungar.*, **15**, (1964), 237–245.
- [9] EPER, M. – SZIRMAI, J.: Coverings with horo- and hyperballs generated by simply truncated orthoschemes, *Submitted manuscript*, (2020).
- [10] FEJES TÓTH, G. - KUPERBERG, W.: Packing and Covering with Convex Sets, Handbook of Convex Geometry Volume B, eds. Gruber, P.M., Willis J.M., pp. 799-860, *North-Holland*, (1983).
- [11] FEJES TÓTH, L.: *Regular Figures*, Pergamon Press, (1964)

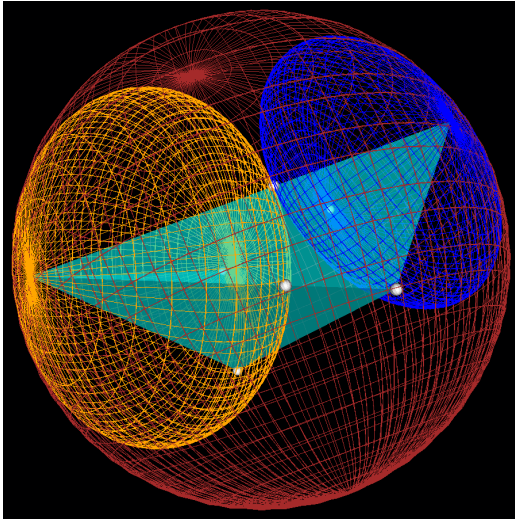


Figure 17: Two horospheres, \mathcal{B}_0 and \mathcal{B}_2 , that touch each other at a point lies on edge A_0A_2 related to tiling $\{\infty, 6, 3, \infty\}$.

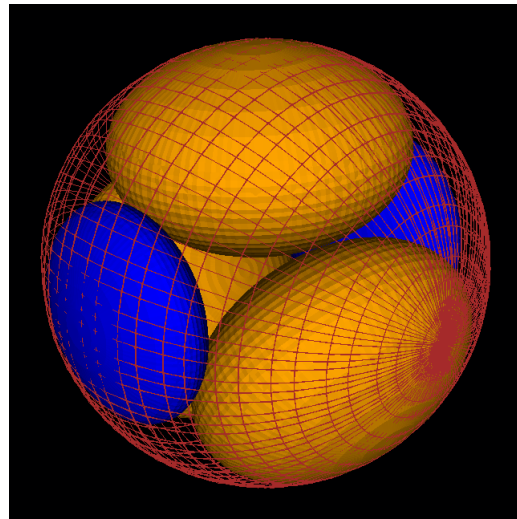


Figure 18: The horosphere configuration (first crown) related to truncated orthoscheme tiling $\{\infty, 6, 3, \infty\}$

- [12] HALES, T. C. – FERGUSON, S. P.: The Kepler conjecture, *Discrete and Computational Geometry*, **36(1)**, (2006), 1–269.
- [13] IM HOF, H.-C.: A class of hyperbolic Coxeter groups, *Expo. Math.*, **3**, (1985), 179–186.
- [14] IM HOF, H.-C.: Napier cycles and hyperbolic Coxeter groups, *Bull. Soc. Math. Belgique*, **42**, (1990), 523–545.
- [15] M. JACQUEMET: The inradius of a hyperbolic truncated n-simplex, *Discrete Comput. Geom.*, **51**, (2014), 997–1016.
- [16] JOHNSON, N.W., KELLERHALS, R., RATCLIFFE, J.G., TSCHANTS, S.T.: The Size of a Hyperbolic Coxeter Simplex, *Transformation Groups*, **4/4** (1999), 329–353.
- [17] KEPLER, J.: *Strena seu de nive sexangula*, Frankfurt, Germany: Tampach (1611) Reprinted in *Gesammelte Werke* (Ed. M. Caspar and F. Hammer, 4 Oxford, England: Clarendon Press (1966)

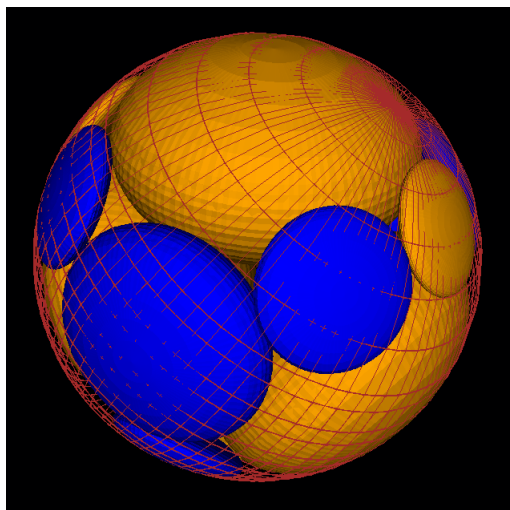


Figure 19: The optimum packing density horosphere configuration (first-second crown) related to the orthoscheme tiling $\{\infty, 6, 3, \infty\}$.

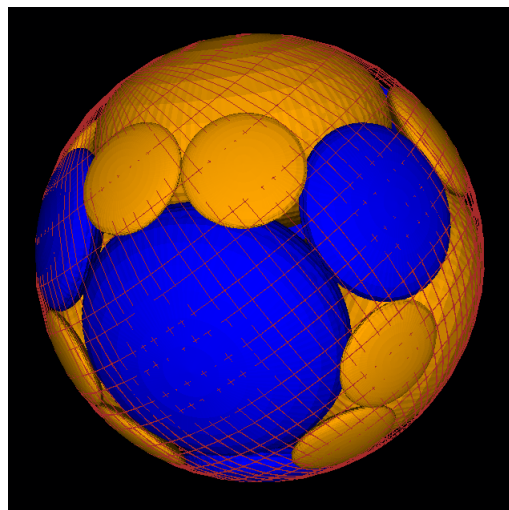


Figure 20: The optimum packing density horosphere configuration (first-third crown) related to the orthoscheme tiling $\{\infty, 6, 3, \infty\}$.

- [18] KELLERHALS, R.: The dilagorithm and volumes of hyperbolic polytopes, *AMS Mathematical Surveys and Monographs*, **37**, (1991), 301–336.
- [19] KELLERHALS, R.: On the volume of hyperbolic polyhedra, *Math. Ann.*, **245**, (1989), 541–569.
- [20] KOZMA, R. T. – SZIRMAI, J.: Optimally dense packings for fully asymptotic Coxeter tilings by horoballs of different types, *Monatsh. Math.*, **168/1**, (2012), 27–47.
- [21] KOZMA, R. T. – SZIRMAI, J.: New lower bound for the optimal ball packing density of hyperbolic 4-space, *Discrete Comput. Geom.*, (2014), DOI: 10.1007/s00454-014-9634-1
- [22] KOZMA, R. T. – SZIRMAI, J.: New horoball packing density lower bound in hyperbolic 5-space, *Geometriae Dedicata*, (2019), DOI: 10.1007/s10711-019-00473-x, arXiv:1809.05411

- [23] KOZMA, R. T. – SZIRMAI, J.: Horoball packing density lower bounds in higher dimensional hyperbolic n -space for $6 \leq n \leq 9$, *Submitted Manuscript*, (2019), arXiv:1907.00595
- [24] KOZMA, R. T. – SZIRMAI, J.: The structure and visualization of optimal horoball packings in 3-dimensional hyperbolic space, *Submitted Manuscript*, (2016), arXiv:1601.03620, (Appendix: <http://homepages.math.uic.edu/rkozma/SVOHP.html>))
- [25] MARSHALL, T. H.: Asymptotic Volume Formulae and Hyperbolic Ball Packing, *Annales Academic Scientiarum Fennica: Mathematica*, **24** (1999), 31–43.
- [26] MOLNÁR, E.: The projective interpretation of the eight 3-dimensional homogeneous geometries, *Beitr. Algebra Geom.*, (1997), **38**, 261–288.
- [27] MOLNÁR, E. – STOJANOVIC, M. – SZIRMAI, J.: Non-fundamental trunc-simplex tilings and their optimal hyperball packings and coverings in hyperbolic space, *Submitted Manuscript* (2020)
- [28] MOLNÁR, E. – SZIRMAI, J.: Top dense hyperbolic ball packings and coverings for complete Coxeter orthoscheme groups, *Publications de L'institut Mathématique*, **103(117)**, (2018), 129–146, DOI: 10.2298/PIM1817129M
- [29] ROGERS, C.A.: Packing and Covering, Cambridge Tracts in Mathematics and Mathematical Physics 54, *Cambridge University Press*, (1964).
- [30] SZIRMAI, J.: Congruent and non-congruent hyperball packings related to doubly truncated Coxeter orthoschemes in hyperbolic 3-space, *Acta Univ. Sapientiae, Mathematica*, **11**, 2 (2019), 437–459.
- [31] SZIRMAI, J.: Horoball packings to the totally asymptotic regular simplex in the hyperbolic n -space, *Aequat. Math.*, **85**, (2013), 471–482, DOI: 10.1007/s00010.012-0158-6.
- [32] SZIRMAI, J.: Horoball packings and their densities by generalized simplicial density function in the hyperbolic space, *Acta Math. Hung.*, **136/1-2**, (2012), 39–55, DOI: 10.1007/s10474-012-0205-8.
- [33] SZIRMAI, J.: Horoball packings related to the 4-dimensional hyperbolic 24 cell honeycomb $\{3, 4, 3, 4\}$, *Filomat*, **32/1**, (2018), 87–100, DOI: 10.2298/FIL1801087S, arXiv:1502.02107.

- [34] SZIRMAI, J.: Hyperball packings in hyperbolic 3-space, *Matematicki Vesnik*, **70/3**, (2018), 211–221, arXiv:1405.0248.
- [35] SZIRMAI, J.: Density upper bound of congruent and non-congruent hyperball packings generated by truncated regular simplex tilings, *Rendiconti del Circolo Matematico di Palermo Series 2*, **67**, (2018), 307–322, DOI: 10.1007/s12215-017-0316-8, arXiv:1510.03208.
- [36] SZIRMAI, J.: Hyperball packings related to octahedron and cube tilings in hyperbolic space, *Contributions to Discrete Mathematics*, **15/2**, (2020), 42–59, arXiv:1803.04948.
- [37] SZIRMAI, J.: The optimal hyperball packings related to the smallest compact arithmetic 5-orbifolds, *Kragujevac Journal of Mathematics*, **40/2**, (2016), 260–270, DOI: 10.5937/KgJMath1602260S, arXiv:1326.4221.
- [38] SZIRMAI, J.: The p -gonal prism tilings and their optimal hypersphere packings in the hyperbolic 3-space, *Acta Math. Hung.*, **111(1-2)**, (2006), 65–76.
- [39] SZIRMAI, J.: The least dense hyperball covering to the regular prism tilings in the hyperbolic n -space, *Ann. Mat. Pur. Appl.*, **195/1**, (2016), 235–248, DOI: 10.1007/s10231-014-0460-0.
- [40] SZIRMAI, J.: Packings with horo- and hyperballs generated by simple frustum orthoschemes, *Acta Math. Hungar.*, **152(2)**, (2017), 365–382, DOI: 10.1007/s10474-017-0728-0.
- [41] SZIRMAI, J.: Decomposition method related to saturated hyperball packings, *Ars Mathematica Contemporanea*, **16**, (2019), 349–358, DOI: 10.26493/1855-3974.14850b1, arXiv:1709.04369.
- [42] SZIRMAI, J.: Upper bound of density for packing of congruent hyperballs in hyperbolic 3-space, *Submitted manuscript*, (2020), arXiv:1812.06785.
- [43] VERMES, I.: Ausfüllungen der hyperbolischen Ebene durch kongruente Hyperzykelbereiche, *Period. Math. Hungar.*, **10/4**, (1979), 217–229.
- [44] VERMES, I.: Über reguläre Überdeckungen der Bolyai-Lobatschewskischen Ebene durch kongruente Hyperzykelbereiche, *Period. Math. Hungar.*, **25/3**, (1981), 249–261.

- [45] VERMES, I.: Bemerkungen zum Problem der dünnsten Überdeckungen der hyperbolischen Ebene durch kongruente Hyperzykelbereiche, *Studia Sci. Math. Hungar.*, **23**, (1988), 1–6.
- [46] YAHYA, A - SZIRMAI, J.: Optimal ball and horoball packings generated by 3-dimensional simply truncated Coxeter orthoschemes with parallel faces. *Submitted manuscript*, (2021), arXiv:2107.08416.